Optimal unsteady convection over a duty cycle for arbitrary unsteady flow under dynamic thermal load

CrossMark

M. Fakoor-Pakdaman *, Mehran Ahmadi, Mehdi Andisheh-Tadbir, Majid Bahrami

Laboratory for Alternative Energy Conversion (LAEC), School of Mechatronic Systems Engineering, Simon Fraser University, Surrey, BC, Canada

ABSTRACT

Developing next generation transient heat exchangers is a transformative technology for efficient thermal management of advanced power electronics and electric machines (APEEM) inside hybrid electric, electric, and fuel cell vehicles as well as renewable energies (wind, solar, tidal). Optimal design criteria for such dynamic heat exchangers should be achieved through addressing internal forced convection with arbitrary flow unsteadiness under dynamic time dependent thermal loads. Exact analytical solutions were obtained for laminar forced-convective heat transfer under arbitrary time-dependent heat flux for steady flow inside a tube (Fakoor-Pakdaman *et al.*, 2014). In this study, the energy equation is solved analytically for arbitrary unsteady flow between parallel plates under dynamic time and position dependent heat flux. As such, laminar pulsating flow between two parallel plates is considered under a harmonic wall heat flux. Exact relationships are obtained to find; (i) temperature distribution for the fluid; (ii) fluid bulk temperature; and (iii) the local and time averaged Nusselt number. New compact relationships are proposed to find the thermal entrance length and the cyclic fully-developed Nusselt number. It is shown that the period of the Nusselt number oscillations is the least common multiple of the periods of the imposed harmonic heat flux and the pulsating flow. We obtained a relationship for the 'cut-off' angular frequency of pulsating flow beyond which the heat transfer does not feel the pulsation. This study also shows that for a given harmonic wall heat flux, there is an optimal pulsating flow velocity, with optimum frequency, which enhances the time averaged Nusselt number by up to 27%.

© 2014 Elsevier Ltd. All rights reserved.

1. Introduction

Optimal design of transient single-phase heat exchangers is a key to developing innovative technology for the next generation advanced power electronics and electric machines (APEEM). APEEM has applications in emerging cleantech systems such as powertrain and propulsion systems of hybrid electric, electric vehicles (EV), and emerging fuel cell vehicles (FCV) [1,2] and green power systems (wind, solar, tidal) [3,4]. Heat generation in APEEM undergo substantial transitions as a direct result of; (i) variable load due to duty cycle, [5–8] and (ii) unsteady coolant flow rate over a duty cycle [9,10]. As such, the heat exchangers/heat sinks associated with APEEM operate periodically over time and never attain a steady-state condition. Conventionally, cooling systems are designed based on a nominal steady-state or a "worst" case scenario, which may not properly represent the thermal behavior

of various applications or duty cycles [7]. Downing and Kojasoy [11] predicted heat fluxes of $150 - 200 \, [\text{W/cm}^2]$ and pulsed transient heat loads up to $400 \, [\text{W/cm}^2]$, for the next-generation insulated gate bipolar transistors (IGBTs) which are used in the design of inverter units of HEVs.

Processes such as start-up, shut down, and pump/fan failure are other typical examples of arbitrary flow unsteadiness for dynamic/transient heat exchangers [12–15]. Besides, depending on the functionality of APEEM over a duty cycle, the coolant flow rate inside the heat exchangers/heat sinks of HE/E/FCV is varying arbitrarily over time [16]. Conventionally mechanical water pumps, directly coupled to the engine, are used in gasoline/diesel vehicles. However, electric vehicles can use variable-speed electric water pump using a separate electric motor and a controller, therefore maintaining an 'optimal' and variable flow rate of the coolant is possible over a driving cycle [9,10]. This provides an opportunity to significantly reduce the parasitic power required for the cooling of HE/E/FCV APEEM and improve the overall efficiency of the vehicle. There are only a few studies in the open literature on this topic. Therefore, there is a pending need for an in-depth understanding of instantaneous thermal characteristics of transient cooling systems

* Corresponding author. Tel.: +1 (778) 782 8538; fax: +1 (778) 782 7514.
  E-mail addresses: mfakoorp@sfu.ca (M. Fakoor-Pakdaman), mahmadi@sfu.ca (M. Ahmadi), mandishe@sfu.ca (M. Andisheh-Tadbir), mbahrami@sfu.ca (M. Bahrami).

Nomenclature

a	Half width of the parallel plates, [m]	
c_p	heat capacity, [J/kg K]	
f	Arbitrary function of time, Eq. (2), $= \frac{u(t)}{u_r}$	
F_n	Eigen values, Eq. (7)	
Fo	Fourier number, $= \alpha t/R^2$	
h	Local heat transfer coefficient, Eq. (23), [W/m^2 K]	
k	Thermal conductivity, (W/m K)	
n	Positive integer, Eq. (7), $= 1,2,3,\ldots$	
Nu_a	Local Nusselt number, Eq. (23), $= ha/k$	
p	Dimemsionless period of temperature fluctuation	
p_1	Dimensionless period of heat flux fluctuation, $= \frac{2\pi}{\omega_1}$	
p_2	Dimensionless period of pulsatile velocity, $= \frac{2\pi}{\omega_2}$	
Pe	Peclet number, $= Re \cdot Pr$	
Pr	Prandtl number, $= v/\alpha$	
q''	Thermal load (Heat flux), [W/m^2]	
Re	Reynolds number, $= 4u_r a/\upsilon$	
t	Time, [s]	
T	Temperature, [K]	
u	Velocity, [m/s]	
x	Axial distance from the entrance of the heated section, [m]	
y	Normal coordinate measured from centerline of parallel plate channel, [m]	
X	Dimensionless axial coordinate, $= 4x/Re \cdot Pr \cdot a$	
Y	Dimensionless normal coordinate, $= y/a$	

Greek letters

α	Thermal diffusivity, [m^2/s]
v	Kinematic viscosity, [m^2/s]
ρ	Fluid density, [kg/m^3]
θ	Dimensionless temperature, $= \frac{T-T_0}{q_r'' a/k}$
φ	Arbitrary function of X and Fo, Eq. (4)
Ω_1	Angular frequency of the heat flux, [rad/s]
Ω_2	Angular frequency of the fluid velocity, [rad/s]
ω_1	Dimensionless angular frequency of the wall heat flux, $= \Omega_1 a^2/\alpha$
ω_2	Dimensionless angular frequency of the fluid velocity, $= \Omega_2 a^2/\alpha$
τ	Dimensionless arbitrary time
ξ	Dummy Fo variable
ζ	Dummy X variable

Subscripts

0	Inlet
m	Mean or bulk value
w	wall
r	Reference value
s	Step heat flux
$Tr.$	Transition

over a given duty cycle. This study is focused on internal forced convection with arbitrary unsteadiness in flow under arbitrary time-varying heat flux. The results of this work will provide a platform for the design, validation and building new intelligent thermal management systems that can actively and proactively control variable-speed electric pumps to circulate a coolant with instantaneous optimal flow rate in APEEM and similar applications.

1.1. Present literature

Siegel [17] pioneered the study on transient internal forced-convective heat transfer. He conducted several studies to investigate the thermal characteristics of steady tube flow under step wall heat flux/temperature [18–20]. Laminar pulsating flow is also addressed in Siegel's study [21] for planar flow in parallel plates under constant heat flux/wall temperature cases. It is shown that quasi-steady assumption does not give an accurate prediction of the thermal characteristics of the pulsating flow for moderate range of pulsation frequency [21]. Guo and Sung [22] addressed the contradictory results of the Nusselt number for pulsating flow in previous published papers; as some researchers had reported heat transfer enhancement, see Refs. [23,24], while heat transfer reduction had been noted in Ref. [25]. They proposed a new model for the time-averaged Nusselt number of laminar pulsating flow under constant wall heat flux. Such definition was introduced based on the time-averaged differences between the tube-wall and fluid-bulk temperatures over a pulsation period. Hemida et al. [26] argued that the small effects of pulsation, which had been noted in previous studies occurred as a result of the restrictive boundary conditions. Wall temperature/heat flux was assumed constant both in space and time. This may affect the heat exchange process, and reduce the effects of pulsation. This shows the necessity to consider more realistic boundary conditions for the tube wall other than constant heat flux or temperature. Less restrictive boundary conditions might manifest into greater

sensitivity to pulsation [26]. This is one of the key issues addressed in the present study. In addition, Brereten and Jiang [27] introduced the idea of fluid flow modulation to increase the time-averaged Nusselt number of pulsating flow under constant heat flux. A summary of literature on laminar pulsating flow is presented in Table 1. Our literature review indicates:

- The existing models for pulsating channel flow are limited to constant wall heat flux/temperature cases.
- Effects of simultaneous oscillation of imposed heat flux and fluid velocity are not investigated in the literature.
- There is no model to determine an optimal velocity frequency for a given harmonic heat flux to maximize the convective heat transfer rate.

To the best of our knowledge, effects of non-constant boundary conditions have not been investigated in the literature neither experimentally nor theoretically. In other words, the answer to the following question is not clear: "can flow pulsation enhance the heat transfer rate in heat exchangers under arbitrary time-dependent loads?"

In our previous studies [31,32], a comprehensive analytical study was performed to predict the thermal characteristics of laminar steady flow under dynamic time-dependent wall heat flux. In the present study, a new analytical model is developed for laminar, single-phase heat transfer between two parallel plates with arbitrary flow unsteadiness under arbitrary time/position dependent wall heat flux. Laminar pulsating flow and harmonic heat flux are considered to obtain exact relationships for: (i) fluid temperature distribution inside the channel; (ii) fluid bulk temperature; and (iii) the Nusselt number. The period of Nusselt number oscillation is obtained under simultaneous oscillation of flow and the imposed wall heat flux. Following Ref. [23], a new definition is introduced to obtain the time-averaged Nusselt number. In addition, optimal pulsating velocity with optimum frequency is found that maximizes

Table 1
Summary of the literature on laminar pulsating channel flow.

Author	Approach	Notes
Siegel and Perlmutter [21]	Analytical (method of characteristics)	√ Reported temperature distribution between two parallel plates √ Covered thermally developing and fully-developed regions × Limited to step wall temperature and heat flux × Nusselt number was defined based on the tube wall and inlet fluid temperature
Hemida et al. [26]	Analytical/numerical (Green's function solution)	√ Reported a closed-form relationship for the temperature distribution in fully-developed region √ Considered different BCs: (i) isoflux; (ii) wall with thermal resistance; (iii) wall with thermal inertia × Treated thermally developing region only numerically
Nield and Kuznetsov [28]	Analytical (perturbation method)	√ Reported transient Nusselt number in circular tubes and parallel plates √ Definition of the Nusselt number similar to [22] × Reported singularity in the solution for $Pr = 1$ × Limited to constant wall heat flux × Limited to oscillations with small amplitudes
Zhao and Cheng [29]	Numerical	√ Proposed a compact relationship for the time averaged Nusselt number for reciprocating flow √ Covered both thermally developing and fully-developed regions × Limited to constant wall temperature
Yan et al. [30]	Analytical/experimental	√ Reported series solutions for temperature distribution and Nusselt number × Limited to constant wall temperature

the heat transfer rate in the channel flow under a given harmonic wall heat flux. An independent numerical study is also performed which compares well with the analytical results; maximum relative difference less than 6%.

To develop the present analytical model, the fluid flow response to a step heat flux is taken into account. A Duhamel's theorem is applied on the thermal response of the fluid flow under the step heat flux, following Ref. [17]. The methodology presented in Ref. [32] is extended to account for arbitrary flow unsteadiness under arbitrary wall heat flux. A harmonic heat flux and pulsating laminar flow are taken into consideration and the thermal characteristics of the fluid flow are determined analytically. Since any time-dependent wall heat flux can be expressed by simple oscillatory functions using a Fourier series transformation [33], the results of this study can be readily applied to determine the pulsating fluid flow response under an arbitrary time-varying heat flux. This approach enables analyzing transient single-phase convective heat transfer under various time-varying conditions, using a superposition technique.

2. Governing equations

Fig. 1 shows fluid flow between two parallel plates with half width of spacing, a, which is thermally insulated in the first sub-region, $x \leqslant 0$, and is heated in the second sub-region, $x > 0$. The entering fluid temperature is maintained at T_0 throughout the heating period. The wall at the second sub-region is given by an arbitrary time-dependent heat flux, $q''(t)$. It should be noted that the second sub-region may be long enough so that the flow can reach thermally fully-developed condition, see Fig. 1. It is intended to determine the evolution of the channel wall temperature, fluid bulk temperature and the Nusselt number as a function of time and space for the entire range of time. Such characteristics are evaluated under dynamic time-dependent heat flux for a fluid flow with arbitrary time-varying velocity.

The assumptions made in deriving the proposed analytical model are listed below:

- Incompressible flow,
- Constant thermo-physical properties,
- Negligible viscous dissipation,
- Negligible axial heat conduction, i.e., $Pe = Re \times Pr \geqslant 10$ [25],
- No thermal energy sources within the fluid,
- No flow reversal in the duct,
- Fluid flow velocity is only a function of time, i.e., slug flow $u = u(t)$.

The slug flow approximation means consideration of one-dimensional velocity distribution, i.e., the fluid is moving through the channel with a mean velocity that can be a function of time. As demonstrated in Refs. [17,20], the slug flow approximation reveals the essential physical behavior of the system, while it enables obtaining exact mathematical solution for various boundary conditions. Using this simplification one can study the effects of various boundary conditions on transient heat transfer without tedious numerical computations [17,20].

The energy equation for a slug flow inside two parallel plates is then become:

$$\frac{\partial T}{\partial t} + u(t)\frac{\partial T}{\partial x} = \alpha\left(\frac{\partial^2 T}{\partial y^2}\right) \tag{1}$$

where the transient velocity between the parallel plates, $u(t)$, in the energy equation can be written as follows:

$$u(t) = u_r \times f(t) \tag{2}$$

Here u_r is a constant reference velocity, and $f(t)$ is an arbitrary function of time. For a special case where $f(t) = 1$, the channel flow velocity is constant slug flow, $u = u_r$, which was investigated in our
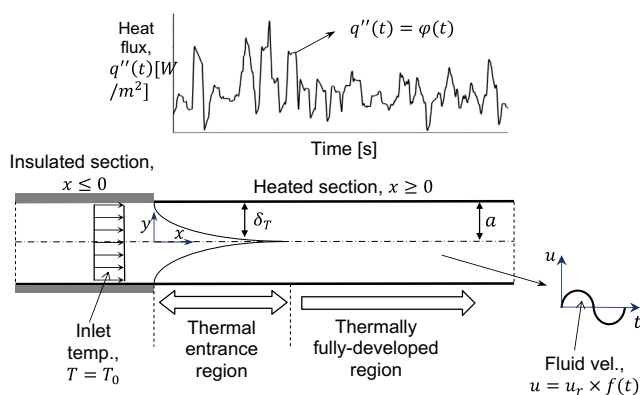

Fig. 1. Schematic of the developing and fully-developed regions, time-dependent wall heat flux and fluid velocity as well as the coordinate system.

previous works [31,32]. As such, the dimensionless form of the energy equation, Eq. (1), then becomes:

$$\frac{\partial \theta}{\partial Fo} + \frac{u}{u_r}\frac{\partial \theta}{\partial X} = \frac{\partial^2 \theta}{\partial Y^2} \tag{3}$$

We define the following dimensionless variables:

$$Fo = \frac{\alpha t}{a^2} \quad X = \frac{4x/a}{Re \cdot Pr} \quad \theta = \frac{T - T_0}{q_r''a/k} \quad Y = \frac{y}{a} \quad Re = \frac{4u_r a}{\upsilon} \quad Pr = \frac{\upsilon}{\alpha}$$

where Fo is the Fourier number and X is the dimensionless axial location that characterizes the flow inside a conduit. As previously mentioned, the goal of this study is to find the transient thermal response of unsteady forced-convective channel flow under arbitrary time-dependent wall heat flux. Therefore, a general wall heat flux is assumed as:

$$q''(X, Fo) = q_r'' \cdot \varphi(X, Fo) \tag{4}$$

where q_r'' is the heat flux amplitude and $\varphi(X, Fo)$ is an arbitrary function of space and time, respectively. Consequently, Eq. (4) is subjected to the following initial and boundary conditions:

$\theta(Y, X, 0) = 0$ Initial condition,

$\theta(Y, 0, Fo) = 0$ Entrance condition,

$(\partial \theta/\partial Y)|_{Y=1} = \frac{q''}{q_r''}(X, Fo) = \varphi(X, Fo)$

    Heat flux at the channel wall for $Fo > 0$,

$(\partial \theta/\partial Y)|_{Y=0} = 0$ Symmetry at the channel centerline. (5)

Although the analysis here are performed for fluid flow between parallel plates, the same methodology can be adopted for other geometries, see Ref. [34] for more detail.

3. Model development

In this section, a new all-time model is developed considering; (i) short-time response and (ii) long-time response. When a slab at uniform temperature T_0 is suddenly subjected to a step heat flux $\Delta q''$ at its surface, the temperature response is [17]:

$$\theta_s = \frac{T - T_0}{q_r''a/k}$$
$$= \frac{\Delta q''}{q_r''}\left[Fo + \frac{3Y^2 - 1}{6} - 2\sum_{n=1}^{\infty}\frac{(-1)^n}{F_n^2} \times \cos(F_n Y) \times \exp\left(-F_n^2 \times Fo\right)\right] \tag{6}$$

where θ_s is the dimensionless temperature of the fluid under a step wall heat flux, F_n are the eigenvalues which can be found by the following relationship:

$$F_n = n\pi \quad n = 1, 2, 3, \ldots \tag{7}$$

The energy equation, Eq. (1), is linear, therefore; a superposition technique can be used to extend the response of the fluid flow for
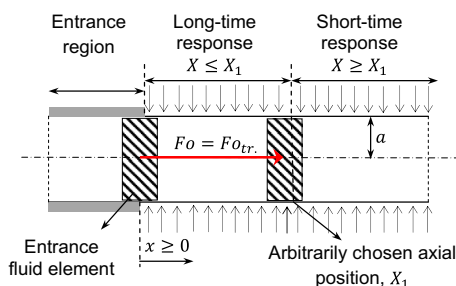
a step heat flux to the other general cases, as discussed in more detail in [35]. Following Siegel [35], by using Duhamel's integral [36], the thermal response for a step heat flux, Eq. (6), can be generalized for arbitrary time/space variations in wall heat flux.

$$\theta = \int_0^{Fo} \frac{q''(\xi)}{q_r''}d\xi + 2\sum_{n=1}^{\infty}(-1)^n \times e^{-F_n^2 \times Fo} \times \cos(F_n Y)$$
$$\times \int_0^{Fo} \frac{q''(\xi)}{q_r''} \times \exp\left(F_n^2 \times \xi\right)d\xi \tag{8}$$

This expression is only valid when the element is initially isothermal, thus the treatment is limited to the cases where the channel was initially isothermal. However, extension to other cases can be achieved by superposition techniques, as discussed in [35].

As shown in Fig. 2, in an Eulerian coordinate system, where the observer is fixed at a given location x along the channel observing the fluid element passes by. For the considered unsteady flow, Eq. (2), it takes some time, $Fo = Fo_{tr.}$, for the fluid element at the entrance to reach a given axial position say X_1. As such, the relationship between the given axial position X_1 and transition time $Fo_{tr.}$ can be formulated as:

$$X_1 = \int_{\xi=0}^{Fo_{tr.}} f(\xi)d\xi \tag{9}$$

Where ξ is the dummy variable, and $Fo_{tr.}$ is the non-dimensional time that takes for the fluid element to reach location X_1. Beyond this distance region, $X \geqslant X_1$, there has not been any penetration of the fluid which was originally outside the channel when the transient began. Hence, the behavior in this region is identical to that of a channel with infinite length in both directions. This means that the convective term in the energy equation, Eq. (1), is zero and a pure transient "heat-conduction" process takes place. This is considered the short-time response of the flow [35]. On the other hand, for $X < X_1$ the observer located at X will see the passing fluid that passed the entrance (insulated) region, when the transient was initiated. This is considered the long-time response of the flow [35]. Therefore, the solution consists of two regions that should be considered separately. The methodology considered in this study is shown schematically in Fig. short-time response, $X \geqslant X_1$

For the sake of generality, we consider a case, where the wall heat flux varies with both time and space, $q''(X, Fo)$. We first consider the region $X \geqslant X_1$. A fluid element that reaches X at time Fo has already passed the heated section at the location $X - \int_{\xi=0}^{Fo} f(\xi)d\xi$ at the beginning of the transient. As this element moves along, it is subjected to the wall heat flux variations in both time and space. At a time τ between 0 and Fo, the element arrives at the location $X - \int_{\xi=\tau}^{Fo} f(\xi)d\xi$. Thus, the heat flux that the element is subjected to at that time is $q''\left(X - \int_{\xi=\tau}^{Fo} f(\xi)d\xi, \tau\right)$. This is substituted into Eq. (8) to find the short-time response for the fluid temperature distribution [35].

$$\theta(X, Fo) = \int_0^{Fo} \frac{q''\left(X - \int_{\xi=\tau}^{Fo} f(\xi)d\xi, \tau\right)}{q_r''}d\tau + 2\sum_{n=1}^{\infty}(-1)^n$$
$$\times \cos(F_n Y) \times \exp\left(-F_n^2 \times Fo\right)$$
$$\times \int_0^{Fo} \frac{q''\left(X - \int_{\xi=\tau}^{Fo} f(\xi)d\xi, \tau\right)}{q_r''} \times \exp\left(F_n^2\tau\right)d\tau \tag{10}$$

It should be noted that according to Eq. (10) when the imposed wall heat flux is only a function of time, $q'' = q''(Fo)$, the short-time thermal response of the fluid flow is independent of the axial position. However, it is a function of time and the characteristics of the imposed wall heat flux.

Fig. 2. The methodology adopted to find the thermal response of the unsteady channel flow under arbitrary time-dependent heat flux.

3.1. Transition time, $X = X_1$

As mentioned earlier the transition time, $Fo = Fo_{tr.}$, for a given axial position, $X = X_1$, can be calculated using Eq. (9). Therefore, the time $Fo = Fo_{tr.}$ separates the short-time from the long-time response for a given axial position.

3.2. Long-time response, $X < X_1$

Now we consider $X < X_1$ region. The element that reaches X at time Fo, has entered the channel at the time Fo_0 and already begun to be heated. This time is found from the following implicit relation:

$$X = \int_{Fo_0}^{Fo} f(\xi)d\xi \qquad (11)$$

Then for this region, we can use Eq. (10) except that the lower limit of the integrals becomes the initial time, Fo_0. Then by analogy with Eq. (10), for $X < X_1$ we have:

$$\theta(X, Fo) = \int_{Fo_0}^{Fo} \frac{q''\left(X - \int_{\xi=\tau}^{Fo} f(\xi)d\xi, \tau\right)}{q_r''} d\tau + 2\sum_{n=1}^{\infty}(-1)^n \times \cos(F_n Y)$$
$$\times \exp\left(-F_n^2 \times Fo\right) \times \int_{Fo_0}^{Fo} \frac{q''\left(X - \int_{\xi=\tau}^{Fo} f(\xi)d\xi, \tau\right)}{q_r''}$$
$$\times \exp\left(F_n^2 \tau\right) d\tau \qquad (12)$$

It should be noted that to find the long-time response, Eqs. (11) and (12) should be solved simultaneously. According to Eq. (12), the long-time thermal response of the fluid flow is a function of time, axial position and the characteristics of the imposed wall heat flux. More detail is presented in Refs. [31,32,37].

4. Heat flux and velocity transients

It is assumed that the transient is initiated by simultaneously changing the fluid flow velocity and channel wall heat flux over time (duty cycle). We develop the present model for a cyclic wall heat flux, as a basic element, noting that the results can be generalized to cover cases with arbitrary time variations in wall heat flux through superposition technique, e.g., Fourier series, Ref. [33]. Throughout this study, the following is considered as a cyclic wall heat flux,

$$\frac{q''}{q_r''}(\Omega_1, t) = [1 + \sin(\Omega_1 t)] \qquad (13)$$

where, $q_r''[W/m^2]$ and Ω_1 [rad/s] are the amplitude and the angular frequency of the imposed harmonic heat flux. The dimensionless form of Eq. (13) is given below:

$$q''(\omega_1, Fo) = q_r''[1 + \sin(\omega_1 \times Fo)] \qquad (14)$$

where $\omega_1 = \frac{\Omega_1 \times a^2}{\alpha}$ is the dimensionless angular frequency of the imposed wall heat flux. In the following sections, the thermal characteristics of unsteady channel flow are investigated under dynamically varying thermal loads for various forms of transient fluid velocity inside the channel. First, laminar pulsating flow is considered for the fluid velocity. Subsequently, a modified form of pulsation is determined to enhance the convective heat transfer rate inside the parallel plates.

4.1. Laminar pulsating flow

In this section, we assume a pulsatile transient velocity which is caused by superimposing pulsation on a mean flow between parallel plates:

$$\frac{u}{u_r} = f(t) = 1 + \sin(\Omega_2 \times t) \qquad (15)$$

where u_r [m/s] and Ω_2 [rad/s] are the amplitude and the angular frequency of the pulsatile flow, respectively. The dimensionless form of Eq. (15) is as follow:

$$\frac{u}{u_r} = 1 + \sin(\omega_2 \times Fo) \qquad (16)$$

where ω_2 is the dimensionless angular frequency of the fluid velocity. At the limit where $\omega_2 = 0$, Eq. (16) yields the constant slug flow inside a conduit. In the following sections, we find the temperature distribution and the Nusselt number for the aforementioned wall heat flux, Eq. (14), and transient velocity, Eq. (16).

4.1.1. Temperature distribution inside the fluid

The dimensionless transition time, $Fo_{tr.}$, for a given axial position, $X = X_1$, can be obtained implicitly by substituting Eq. (16) into Eq. (9) as follows:

$$X_1 = Fo_{tr.} + \frac{1}{\omega_2}[1 - \cos(\omega_2 \times Fo_{tr.})] \qquad (17)$$

Short-time response, $X \geqslant X_1$:

$$\theta(X, Fo, \omega_1) = Fo + \frac{1}{\omega_1}[1 - \cos(\omega_1 Fo)] + \frac{3Y^2 - 1}{6} + 2\sum_{n=1}^{\infty}(-1)^n$$
$$\times \cos(F_n Y) \times \left\{ \begin{array}{l} \frac{F_n^2 \times \sin(\omega_1 Fo) - \omega_1 \times \cos(\omega_1 Fo) + \omega_1 \times \exp\left(-F_n^2 \times Fo\right)}{\omega_1^2 + F_n^4} \\ -\frac{\exp\left(-F_n^2 \times Fo\right)}{F_n^2} \end{array} \right\} \qquad (18)$$

Long-time response, $X \leqslant X_1$:

$$\theta(X, Fo, \omega_1) = Fo - Fo_0 + \frac{1}{\omega_1}[\cos(\omega_1 Fo_0) - \cos(\omega_1 Fo)]$$
$$+ \frac{3Y^2 - 1}{6} + 2\sum_{n=1}^{\infty}(-1)^n \times \cos(F_n Y)$$
$$\times \left\{ \begin{array}{l} \frac{F_n^2 \times \sin(\omega_1 Fo) - \omega_1 \times \cos(\omega_1 Fo)}{\omega_1^2 + F_n^4} + \\ \frac{\left\{-F_n^2 \times \sin(\omega_1 Fo_0) + \omega_1 \times \cos(\omega_1 Fo_0)\right\} \times \exp\left[F_n^2 \times (Fo_0 - Fo)\right]}{\omega_1^2 + F_n^4} - \\ \frac{\exp\left[F_n^2 \times (Fo_0 - Fo)\right]}{F_n^2} \end{array} \right\} \qquad (19)$$

Where Fo_0 is found from the following relationship:

$$X_1 = Fo - Fo_0 + \frac{1}{\omega_2}[\cos(\omega_2 \times Fo_0) - \cos(\omega_2 \times Fo)] \qquad (20)$$

In this study, we considered the first 60 terms of the series solutions, using more terms does not affect the solution up to four decimal digits.

4.1.2. Fluid bulk temperature

The bulk temperature of a constant-property fluid for the slug flow condition can be obtained by the following relationship, Ref. [38]:

$$\theta_m(X, Fo) = \int_0^1 \theta(Y, X, Fo)dY \qquad (21)$$

Substituting Eqs. (18) and (19) into Eq. (21), the short-time and long-time fluid bulk temperature can be obtained as follows:

$$\theta_m(X, Fo, \omega_1) = \begin{cases} Fo + \frac{1}{\omega_1}[1 - \cos(\omega_1 Fo)] & X \geqslant X_1 \\ Fo - Fo_0 + \frac{1}{\omega_1}\{\cos(\omega_1 Fo_0) - \cos(\omega_1 Fo)\} & X < X_1 \end{cases} \qquad (22)$$

4.1.3. Nusselt number

In most Siegel works [16–21], the transient thermal behavior of a system is evaluated based on the dimensionless wall heat flux considering the difference between the local tube wall and the initial fluid temperature. We are of the opinion that an alternative definition of the local Nusselt number has a more 'physical' meaning, i.e., based on the local difference between the channel wall and the fluid bulk temperature at each axial location; this is consistent with Refs. [22,38]. It should be emphasized that the definition of the Nusselt number is an arbitrary choice and will not alter the final results.

$$Nu_a = \frac{ha}{k} = \frac{1 + \sin(\omega_1 Fo)}{\theta_w - \theta_m} \tag{23}$$

where Nu_a is the local Nusselt number and θ_w is the dimensionless wall temperature obtained from Eqs. (18) and (19) with $Y = 1$. Therefore, the short-time and long-time Nusselt numbers are obtained as follows:

Short-time Nusselt number, $X \geqslant X_1$:

$$Nu_a(Fo, \omega_1) = \frac{1 + \sin(\omega_1 Fo)}{\frac{1}{3} + 2\sum_{n=1}^{\infty} \left\{ \frac{F_n^2 \times \sin(\omega_1 Fo) - \omega_1 \times \cos(\omega_1 Fo) + \omega_1 \times \exp\left(-F_n^2 \times Fo\right)}{\omega_1^2 + F_n^4} - \frac{\exp\left(-F_n^2 \times Fo\right)}{F_n^2} \right\}} \tag{24}$$

Long-time Nusselt number, $X < X_1$:

$$Nu_a(X, Fo, \omega_1) = \frac{1 + \sin(\omega_1 Fo)}{\frac{1}{3} + 2\sum_{n=1}^{\infty} \left\{ \frac{F_n^2 \times \sin(\omega_1 Fo) - \omega_1 \times \cos(\omega_1 Fo) +}{\omega_1^2 + F_n^4} + \frac{\left\{-F_n^2 \times \sin(\omega_1 Fo_0) + \omega_1 \times \cos(\omega_1 Fo_0)\right\} \times \exp\left[F_n^2 \times (Fo_0 - Fo)\right]}{\omega_1^2 + F_n^4} - \frac{\exp\left[F_n^2 \times (Fo_0 - Fo)\right]}{F_n^2} \right\}} \tag{25}$$

As previously mentioned in Section 3, the short-time Nusselt number is only a function of time and angular frequency. However, the long-time Nusselt number is a function of time, angular frequency, and the axial location. In addition, Fo_0 is found by Eq. (20). The time-averaged Nusselt number over a period of fluctuation is defined in this study as follows:

$$\overline{Nu_a}(X) = \frac{1}{p} \int_{Fo=0}^{p} Nu_a \, dFo \tag{26}$$

where $\overline{Nu_a}(X)$ is the local time-averaged Nusselt number and p is the period of temperature oscillation inside the fluid. The latter depends on the period of heat flux, $p_1 = \frac{2\pi}{\omega_1}$, and the fluid flow pulsation, $p_2 = \frac{2\pi}{\omega_2}$. This will be discussed in detail in Section 6.

4.2. Optimum transient velocity

An optimum pulsating velocity can be defined to increase the time-averaged Nusselt number of a pulsating flow compared to its associated constant slug flow condition, see Ref. [27]. This will be discussed in detail in Section 6. This optimal pulsating velocity is considered as follows:

$$\frac{u}{u_r} = 1 + |\sin(\omega_2 \times Fo)| \tag{27}$$

For this transient velocity, the temperature distribution is obtained by Eqs. (18) and (19), while the Nusselt number can be calculated by Eqs. (24) and (25). However, modified forms of Eqs. (9) and (11) should be solved to find $Fo_{tr.}$ and Fo_0 implicitly for a given axial position, $X = X_1$, over time. As a result, Eq. (28) indicates the implicit relationship for dimensionless transition time, $Fo = Fo_{tr.}$, for an arbitrarily chosen axial position, $X = X_1$.

$$X_1 = \int_{\zeta=0}^{Fo_{tr.}} [1 + |\sin(\omega_2 \zeta)|] d\zeta \tag{28}$$

In addition, to find the long-time response the following implicit relationship can be used to find the parameter Fo_0, for an arbitrary axial position, $X = X_1$.

$$X_1 = \int_{\zeta=Fo_0}^{Fo} [1 + |\sin(\omega_2 \zeta)|] d\zeta \tag{29}$$

5. Numerical study

In this section, an independent numerical simulation of the axisymmetric flow inside parallel plates is conducted using the commercial software, ANSYS® Fluent [20]. User defined codes (UDFs) are written to apply the dynamic heat flux boundary conditions on the channel wall, Eq. (14), and the transient velocity between the parallel plates, Eq. (16). The assumptions stated in Section 2 are used in the numerical analysis. Grid independency of the results is tested for three different grid sizes, 20×100, 40×200, as well as 80×400, and 40×200 is selected as the final grid size, since the maximum difference in the predicted values for the fluid temperature by the two latter grid sizes is less than 2%. Air is selected as the working fluid for the numerical simulations. The geometrical and thermal properties used in the baseline case for the numerical simulation are listed in Table 2. The maximum relative difference between the analytical results and the numerical data is less than 6%, which are discussed in detail in Section 6.

6. Results and discussion

Variations of the dimensionless channel wall temperature against the Fo number, Eqs. (18) and (19), for three axial positions along the channel are shown in Fig. 3 and compared with the numerical data (markers) obtained in Section 5 of this study. The imposed wall heat flux is assumed to be constant over time, $q'' = q''_r = \text{const.}$, and the fluid velocity fluctuates harmonically over time, $U(Fo) = \frac{u}{u_r} = 1 + \sin(\pi \times Fo)$, respectively.

One can conclude the following from Fig. 3:

- The present model predicts an abrupt transition between the short-time and long-time responses. The numerical results, however, indicate a smoother transition between the responses. This causes the numerical data to deviate slightly from the analytical results as the long-time response begins. The maximum relative difference between the present analytical model and the numerical data occurs at this transition and is less than 6%.
- The abrupt transition between the short- and long-time responses occurs as a result of the limitations of the method of characteristics which is used to solve the energy equation, Eq. (3). More detail is presented in Ref. [31].
- There is an initial transient period of pure conduction during which all of the curves follow along the same line, $Fo \leqslant Fo_{tr.}$.
- When $Fo = Fo_{tr.}$, each curve stems from the common line, i.e., pure conduction response, and moves towards a steady oscillatory behavior at long-time response, Eqs. (18) and (19). The wall temperature increases at larger X values, as expected, because of the increase in the fluid bulk temperature in the axial direction.
- When the heat flux is constant and the fluid velocity is fluctuating over time, the temperature field fluctuates with the same angular frequency. It is also the case when the velocity is constant and the wall heat flux is fluctuating harmonically over

Table 2
Values of the thermal and geometrical properties used for the baseline case in the present numerical simulation.

Properties	Density, ρ[kg/m³]	Dynamic viscosity, μ[Pa s]	Thermal conductivity, k[W/m/K]	Thermal capacity, c_p[J/kg/K]	Channel half width, a[m]
Values	1.225	1.7894E-5	0.0242	1006.43	0.05

$q_r'' = 100$ [W/m²], $u_r = 0.02$ [m/s], $T_0 = 300$ [K]
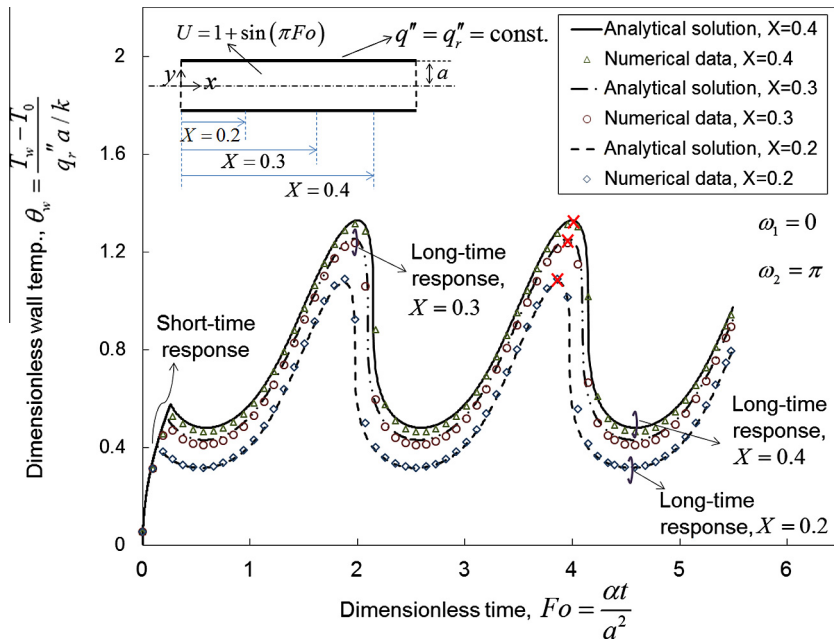
Fig. 3. Channel wall temperature against the dimensionless time, Eqs. (18) and (19), for a few axial positions along the channel, and comparison with the obtained numerical data (markers), when q'' = const. and $U = 1 + \sin(\pi \times Fo)$.
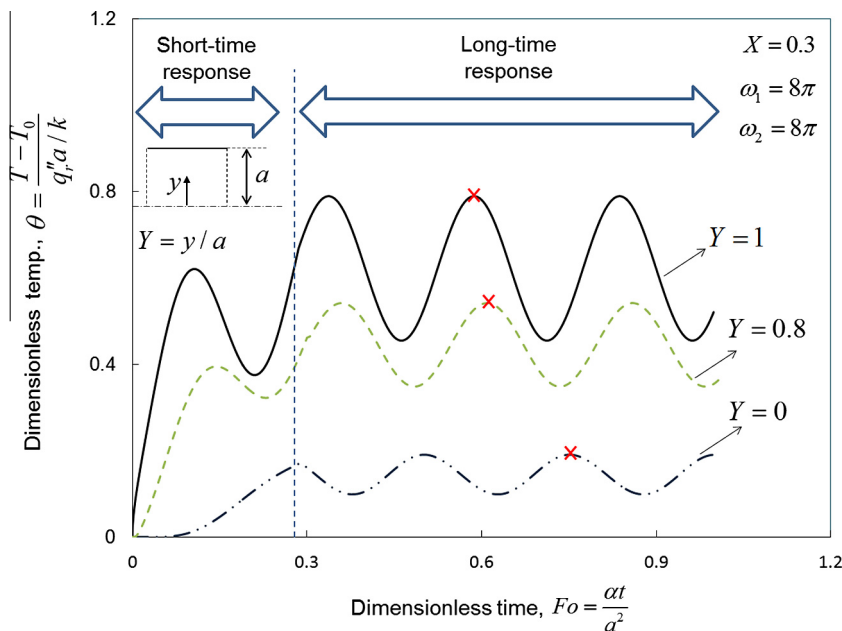
Fig. 4. Variations of the dimensionless fluid temperature at an arbitrarily-chosen axial position of $X = 0.3$ at different vertical positions across the channel against the Fo number where $q''/q_r'' = 1 + \sin(8\pi \times Fo)$ and $U(Fo) = u/u_r = 1 + \sin(8\pi \times Fo)$.

time, see Ref. [32] for more detail. The angular frequency of the temperature field inside the fluid when both heat flux and velocity are fluctuating over time will be discussed later in this section.

- The shift between the peaks of the temperature profile is marked at different axial positions. This shows a "thermal lag" (inertia) of the fluid flow, which increases in x-direction towards the downstream of the channel.

Variations of the dimensionless temperature inside the fluid for a few vertical positions across the channel against the dimensionless time are depicted in Fig. 4. The axial position is arbitrarily fixed at $X = 0.3$; the imposed heat flux, and the fluid velocity are varying harmonically over time, i.e., $q''/q_r'' = 1 + \sin(8\pi \times Fo)$ and $U(Fo) = 1 + \sin(8\pi \times Fo)$, respectively.

The following can be concluded from Fig. 4:

- At any given axial position, there is an initial transient period, which can be considered as pure conduction, i.e., the short-time response for $Fo \leqslant Fo_{tr.}$. However, as previously mentioned, each axial position shows a steady oscillatory behavior for $Fo > Fo_{tr.}$ at the long-time response.
- Regarding Eq. (17), for a given axial position of $X = 0.3$, the long-time response begins at $Fo_{tr.} = 0.28$, and shows the same behavior at all-time thereafter.
- The shift between the peaks of the temperature profile is marked at different vertical positions. This shows a "thermal lag" (inertia) of the fluid flow, which increases towards the centerline of the channel in the y-direction. In fact, this happens due to the thermal inertia of the fluid, and the harmonic heat flux imposed on the channel wall, $q''/q_r'' = 1 + \sin(8\pi \times Fo)$.
- At a given axial position, the fluid temperature increases in radial locations closer to the channel wall. This occurs since; (i) the heat flux is imposed at the channel wall; and (ii) the fluid thermal inertia is less in regions near the wall.

Fig. 5 shows the variations of the local Nusselt number versus the Fourier number for three axial positions along the channel. The imposed wall heat flux and the fluid velocity are considered to vary harmonically over time, i.e., $\frac{q''}{q_r''} = 1 + \sin(8\pi \times Fo)$ and $U = 1 + \sin(8\pi \times Fo)$, respectively.

The following can be concluded from the trends in Fig. 5:

- At early times, before the initiation of the long-time response, "pure-conduction-like" heat transfer occurs, and the Nusselt number of all axial positions is only a function of time.
- The troughs of the Nusselt number at different axial positions are the same corresponding to the times, when the wall heat flux is zero.
- The values of the Nusselt number decrease at higher axial locations, i.e., further downstream. This is attributed to the boundary layer growth which insulates the channel wall, and reduces the rate of the heat transfer.
- For axial positions $X \geqslant 0.3$, the Nusselt number varies less than 4% with an increase in axial position. This indicates the existence of a fully-developed region similar to that of the constant slug flow under dynamic thermal load, see Ref. [32]. At $X = 0.3$, the boundary layers on the channel wall merge and the Nusselt number reaches its cyclic fully-developed value.
- In thermal fully-developed region: defined as the region where $X \geqslant 0.3$, the Nusselt number for pulsating channel flow under harmonic heat flux does not vary with the axial location any further. However, it can be an arbitrary function of time and the characteristics of the imposed heat flux.
- The main characteristic of the defined fully-developed region, $X \geqslant 0.3$, is the fact that the pulsation effect is fully damped. As such, the fully-developed Nusselt number for pulsating flow with a given angular frequency yields that of the constant slug flow condition.
- Using a curve fitting technique, the following compact relationship is developed in this study. This relationship can be used to find the fully-developed Nusselt number for laminar pulsating flow under dynamic heat flux for $\pi \leqslant \omega_1 \leqslant 10\pi$, $\pi \leqslant \omega_2 \leqslant 15\pi$, and $X \geqslant 0.3$. The maximum relative difference between the exact series solution, Eq. (25), and Eq. (30) is less than 10%.

$$Nu_a = \frac{1 + \sin(\omega_1 \times Fo)}{\frac{1}{3} + 0.16 \times \sin(\omega_1 \times Fo - 0.7)} \tag{30}$$
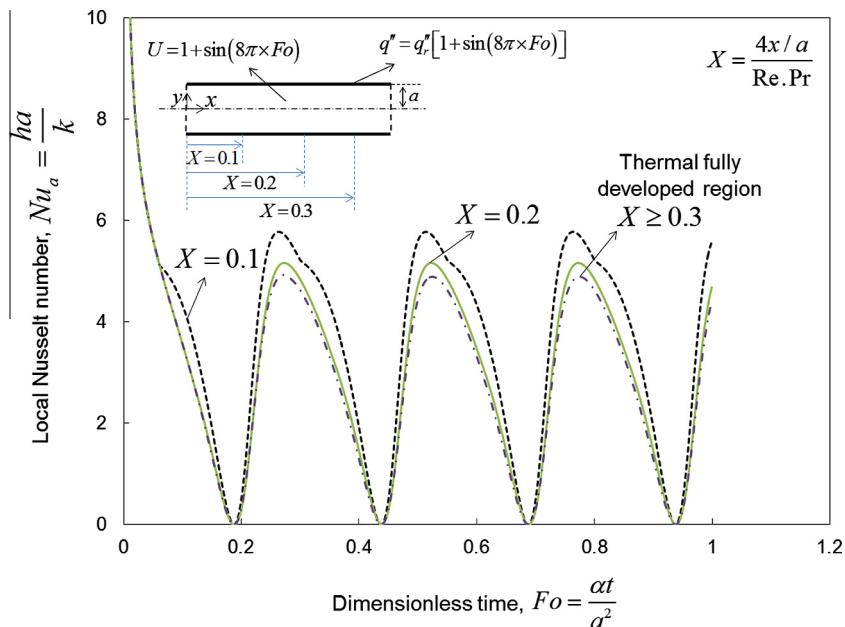

Fig. 5. Variations of the local Nusselt number against the Fourier number at different axial positions along the channel, when $\frac{q''}{q_r''} = 1 + \sin(8\pi \times Fo)$ and $U = 1 + \sin(8\pi \times Fo)$.
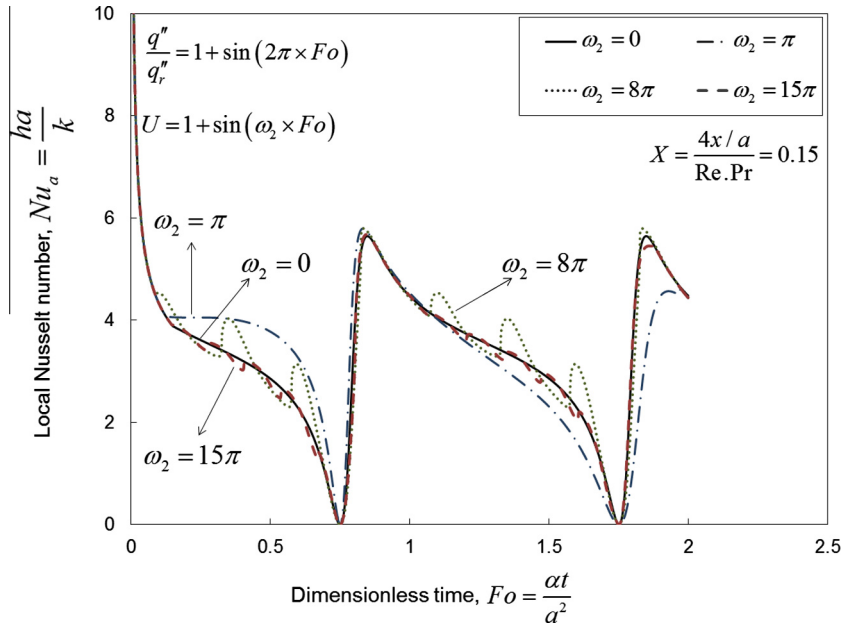
Fig. 6. Variations of the local Nusselt number versus dimensionless time (*Fo* number), for different values of the pulsation frequency ω_2, where $\frac{q''}{q_r''} = 1 + \sin(2\pi \times Fo)$.

Depicted in Fig. 6 are the variations of the local Nusselt number against the dimensionless time, *Fo*, for different values of the pulsation angular frequency, ω_2. The imposed wall heat flux is assumed to vary harmonically over time, i.e., $\frac{q''}{q_r''} = 1 + \sin(2\pi \times Fo)$. The results are shown for an arbitrary axial position, *X* = 0.15. The trends for other axial positions are similar.

The following conclusions can be drawn from Fig. 6:

- The local Nusselt number is zero at times when the imposed wall heat flux is zero.
- When the periods of the heat flux and pulsating velocity are $p_1 = \frac{2\pi}{\omega_1}$ and $p_2 = \frac{2\pi}{\omega_2}$, respectively, the period of fluid temperature is the least common multiple (LCM) of the periods. As such, as shown in Fig. 6, when $\omega_1 = 2\pi$ and $\omega_2 = 8\pi$, the period of the long-time temperature inside the fluid is:

$$\begin{cases} p_1 = \frac{2\pi}{\omega_1} = 1 \\ p_2 = \frac{2\pi}{\omega_2} = \frac{1}{4} \end{cases} \Rightarrow p = LCM(p_1, p_2) = 1 \qquad (31)$$

- For a pulsating velocity with high angular frequency, the fluid does not follow the cycles of the velocity due to its thermal inertia, i.e., the fluctuations are filtered out. Therefore, for high angular frequencies, the flow acts as if the fluid velocity is constant at the average value associated with zero frequency for the sinusoidal term of the pulsating velocity, for this case. This is called the "cut-off" pulsation frequency.
- Dimensionless cut-off pulsation frequency: defined in this study as the angular frequency beyond which the pulsating Nusselt number lies within ± 5% of that of steady slug flow condition. As such, for a pulsating flow between parallel plates subjected to harmonic wall heat flux, $\omega_2 = \frac{\Omega_2 \times a^2}{\alpha} = 15\pi$ is the cut-off angular frequency.
- Regarding Eq. (15), the dimensionless cut-off frequency is a function of pulsation angular frequency, Ω_2 [rad/s], channel half width, $a[m]$, and fluid thermal diffusivity, $\alpha \left[\frac{m^2}{s}\right]$.

Fig. 7 shows the variations of the local Nusselt number at an arbitrarily chosen axial position, *X* = 0.1, against the Fourier number.

Pulsating flow, $U = 1 + \sin(\pi/8 \times Fo)$, and constant slug flow, $U = \frac{u}{u_r} = 1$, are considered for the fluid velocity. In addition, the imposed wall heat flux is chosen arbitrarily as $\frac{q''}{q_r''} = 1 + \sin(\pi \times Fo)$. The following conclusions can be drawn from Fig. 7:

- For a constant velocity inside the conduit, the long-time Nusselt number fluctuates with the angular frequency of the imposed heat flux. In mathematical notation, $\omega_2 = 0 \Rightarrow p = p_1 = \frac{2\pi}{\omega_1} = 2$.
- For the considered pulsating velocity, $p_2 = \frac{2\pi}{\omega_2} = 16$, and the period of the imposed wall heat flux is, $p_1 = 2$. Therefore the period of fluctuations of the local Nusselt number for this instance is: $p = LCM(2,16) = 16$. The results will be repeated periodically from that time thereafter, $Fo \geqslant 16$.
- Over the first half cycle of the pulsation, $Fo \leqslant \frac{p_2}{2}$, the Nusselt number of pulsating velocity is higher than that of constant slug flow. In fact, this happens since during the first half cycle the sinusoidal term of pulsating velocity is positive. As a result, the flow rate inside the conduit is higher than that of constant slug-flow case.
- On the other hand, over the second half cycle, $\frac{p_2}{2} \leqslant Fo \leqslant p_2$, the sinusoidal term of the pulsating velocity becomes negative which in turn decreases the local Nusselt number of the pulsating flow compared to its constant slug-flow case.
- The time averaged *Nu* number is the area under the local Nu curves presented in Fig. 7, see Eq. (26). As such, over the defined period of fluctuation, $0 \leqslant Fo \leqslant p$, the time-averaged *Nu* number for pulsating flow is equal to that of constant slug-flow case.
- Modulating the pulsating velocity to maintain the oscillatory term positive can remarkably enhance the local Nusselt number at a given axial position, see Ref. [27]. This is called the "optimal pulsating velocity" which can be defined as, $U = \frac{u}{u_r} = 1 + |\sin(\omega_2 Fo)|$.

Fig. 8 depicts the variations of the local *Nu* number against the *Fo* number for different values of angular frequencies of the "optimal pulsating velocity", i.e., $U = \frac{u}{u_r} = 1 + |\sin(\omega_2 Fo)|$. The axial position is arbitrarily chosen at *X* = 0.1, and the imposed heat flux is assumed as, $\frac{q''}{q_r''} = 1 + \sin(\pi \times Fo)$.
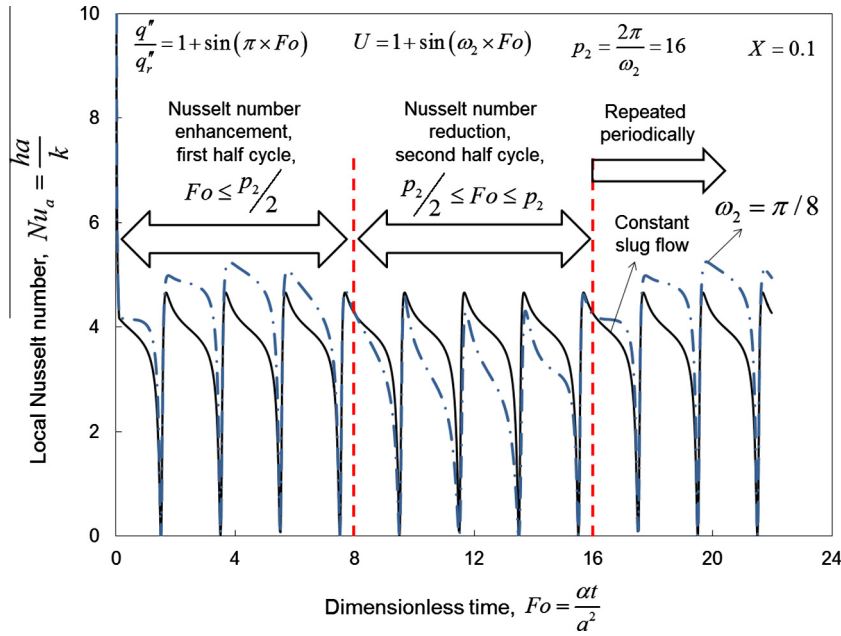
The following can be concluded from Fig. 8:

Fig. 7. Variations of the local Nusselt number at a given axial position, $X = 0.1$, against dimensionless time when $U = 1 + \sin\left(\frac{\pi}{8} \times Fo\right)$, and comparison with constant slug flow condition, $U = \frac{u}{u_r} = 1$.
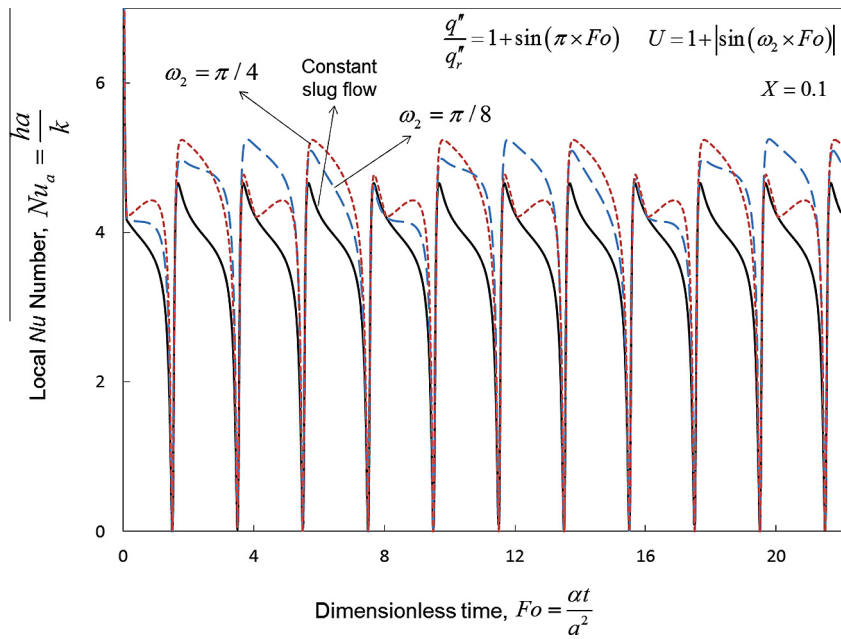

Fig. 8. Variations of the local Nu number against the Fo number for different angular frequencies where $U = 1 + |\sin(\omega_2 Fo)|$ and $\frac{q''}{q''_r} = 1 + \sin(\pi \times Fo)$.

- Irrespective of the angular frequency over a given period of time, the Nusselt number of the optimal pulsating flow is higher than that of the constant slug flow case.
- Comparing Figs. 7 and 8, it is evident that the local Nu number reduction which happened for the second half cycle of pulsating flow, $U = 1 + \sin(\omega_2 \times Fo)$, does not exist when using optimal pulsating flow, i.e., $U = 1 + |\sin(\omega_2 Fo)|$.
- As previously mentioned, the time averaged Nusselt number is the area below the local Nu curves presented in Fig. 8. Since this area is not the same for different angular frequencies, the time averaged Nusselt number depends on the angular frequency of the optimal pulsating flow.
- For a given harmonic wall heat flux, there is an "optimum angular frequency" which maximizes the time-averaged Nu number

of optimal pulsating flow, $U = 1 + |\sin(\omega_2 Fo)|$, compared to its constant slug flow case, $U = \frac{u}{u_r} = 1$.

Fig. 9 shows the enhancement of time averaged Nusselt number as a result of using the optimal pulsating flow compared to the corresponding steady slug flow inside a duct. Three axial positions along the duct are chosen arbitrarily to show the time averaged Nu number enhancement. Note that the heat transfer enhancement is defined by the following relationship:

$$\Delta \overline{Nu} = \overline{Nu}_{\omega_2 \neq 0} - \overline{Nu}_{\omega_2 = 0} \tag{32}$$

where $\Delta \overline{Nu}$ is the enhancement of the time-averaged Nu. In addition, $\overline{Nu}_{\omega_2 \neq 0}$, and $\overline{Nu}_{\omega_2 = 0}$ are the time-averaged Nu for pulsating flow,
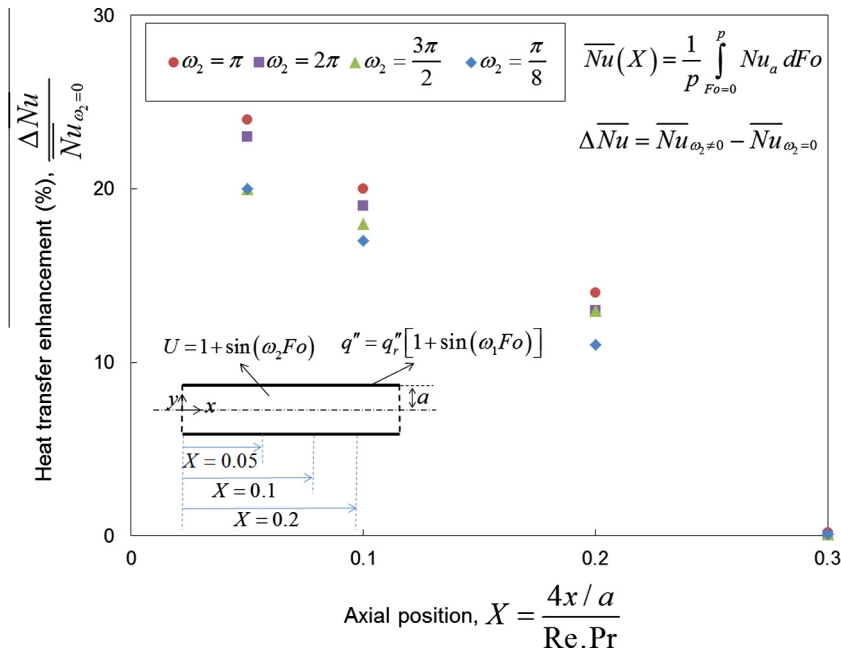
Fig. 9. Time averaged Nusselt number enhancement at different axial positions along the duct for various pulsation frequencies where $q'' = q_r''[1 + \sin(\pi Fo)]$.

and its corresponding steady slug flow, respectively. As previously mentioned, the time averaged Nu in this study is defined over a period of fluctuation $0 \leqslant Fo \leqslant p$, see Eq. (26).

The following can be concluded from Fig. 9:

- Irrespective of angular frequency, the optimal pulsating flow, $U = 1 + |\sin(\omega_2 Fo)|$, increases the time averaged Nu number compared to constant slug flow condition.
- The time averaged Nusselt number increases up to 27% at the axial position, $X = 0.05$, compared to the corresponding constant slug-flow inside the duct.
- There is an "optimum frequency" which maximizes the Nu number enhancement. This value depends on the frequency of the imposed harmonic wall heat flux. For instance, when $\omega_1 = \pi$ this optimum value is, $\omega_{2,opt.} = \pi$.
- Downstream of the channel, the pulsation effects decrease; as a result, the heat transfer enhancement drops. For $X \geqslant 0.3$ the effects of pulsation are completely damped, and there is no heat transfer enhancement in the channel. Therefore, it is beneficial to design heat exchangers considering this length.
- The cost of using a controlled unsteady flow to enhance the Nusselt number is an increase in the input pumping power. This power requirement is a function of pressure gradient and flow rate in unsteady flow. The present model provides a platform for optimization analyses needed to design cost-effective 'green' cooling systems.

7. Conclusion

A new all-time range analytical model is developed to predict the thermal characteristics of pulsating channel flow under dynamic time-dependent heat flux and can be used to evaluate: (i) temperature distribution inside the fluid; (ii) fluid bulk temperature; and (iii) the Nusselt number. Compact relationships are developed to obtain the thermal entrance length and fully-developed Nusselt number. For the first the concept of optimal pulsating flow with an optimum frequency is introduced to maximize the time averaged Nusselt number. The highlights of this study can be listed as follows:

- The period of the temperature and Nusselt fluctuation inside the fluid is the least common multiple of the periods of the heat flux and the pulsating flow.
- There is a cut-off angular frequency for pulsating flow, i.e. $\omega_2 = 15\pi$, beyond which the Nusselt number yields that of the constant slug-flow condition.
- Effects of pulsation along the duct decrease as the thermal boundary layer grows. As such, for $X \geqslant 0.3$ the pulsation effects are fully-damped and the fluid flow reaches thermally fully-developed condition.
- There is an optimal pulsating flow with an optimum frequency which increases the heat transfer rate remarkably compared to the constant flow condition. Heat transfer enhancements of up to 27% can be achieved at the thermal entrance region.
- The optimum frequency depends on the angular frequency of the imposed heat flux. In other words, for an imposed harmonic wall heat flux, there is an optimum value for the pulsation frequency which maximizes the heat transfer enhancement.

The question whether the flow pulsation increases or reduces the heat transfer rate of convective cooling systems under time dependent thermal load is answered here as follows: the time averaged Nu number of pulsating flow is equal to that of steady flow over a period of fluctuation. However, within the context of "optimal velocity" up to 27% heat transfer enhancement is noted compared to steady slug flow case.

Conflict of interest

None declared.

References

[1] M. Marz, A. Schletz, Power electronics system integration for electric and hybrid vehicles, in: 6th Int. Conf. Integr. Power Electron. Syst., 2010: Paper 6.1.

[2] K. Chau, C. Chan, C. Liu, Overview of permanent-magnet brushless drives for electric and hybrid electric vehicles, IEEE Trans. Ind. Electron. 55 (2008) 2246–2257.

[3] J. Garrison, M. Webber, Optimization of an integrated energy storage scheme for a dispatchable wind powered energy system, in: ASME 2012 6th Int. Conf. Energy Sustain. Parts A B San Diego, California, USA, 2012, pp. 1009–1019.

[4] J. Garrison, M. Webber, An integrated energy storage scheme for a dispatchable solar and wind powered energy system and analysis of dynamic parameters, Renew. Sustain. Energy. 3 (2011) 1–11.

[5] I. Mudawar, Assessment of high-heat-flux thermal management schemes, IEEE Trans. Components Packag. Technol. 24 (2001) 122–141.

[6] M.R.O. Panão, A.M. Correia, A.L.N. Moreira, High-power electronics thermal management with intermittent multijet sprays, Appl. Therm. Eng. 37 (2012) 293–301.

[7] M. O'Keefe, K. Bennion, A comparison of hybrid electric vehicle power electronics cooling options, in: Veh. Power Electron. Cool. Options, 2007, pp. 116–123.

[8] T.J. Lu, Thermal management of high power electronics with phase change cooling, Int. J. Heat Mass Transfer 43 (2000) 2245–2256.

[9] D.H. Lim, S.C. Kim, M.S. Kim, Thermal analysis of an electric water pump for internal combustion engine vehicles, Int. J. Autom. Technol. 14 (2013) 579–585.

[10] J.-S. Park, B.-G. Gu, J.-H. Choi, I.-S. Jung, Development of BLDC motor drive for automotive water pump systems, J. Int. Counc. Electr. Eng. 1 (2011) 395–399.

[11] R. Scott Downing, G. Kojasoy, Single and two-phase pressure drop characteristics in miniature helical channels, Exp. Therm. Fluid Sci. 26 (2002) 535–546.

[12] H. Bhowmik, C.P. Tso, K.W. Tou, Thermal behavior of simulated chips during power-off transient period, Packag. Technol. 65 (2003) 497–500.

[13] J.A. Clarck, V.S. Arpaci, Dynamic response of heat exchangers having internal heat sources, Trans. ASME 80 (1958) 612–624.

[14] J.A. Clarck, V.S. Arpaci, Dynamic response of heat exchangers having internal heat sources- Part II, Trans. ASME 80 (1958) 625–634.

[15] E.M. Sparrow, F.N. De Farias, Unsteady heat transfer in ducts with time-varying inlet temperature and participating walls, Int. J. Heat Mass Transfer 11 (1968) 837–853.

[16] K. Bennion, M. Thornton, Integrated vehicle thermal management for advanced vehicle propulsion technologies, SAE(2010-01-0836), 2010.

[17] R. Siegel, Transient heat transfer for laminar slug flow in ducts, Appl. Mech. 81 (1959) 140–144.

[18] E.M. Sparrow, R. Siegel, Thermal entrance region of a circular tube under transient heating conditions, in: Third U.S. Natl. Congr. Appl. Mech., 1958, pp. 817–826.

[19] R. Siegel, E.M. Sparrow, Transient heat transfer for laminar forced convection in the thermal entrance region of flat ducts, Heat Transfer 81 (1959) 29–36.

[20] R. Siegel, Heat transfer for laminar flow in ducts with arbitrary time variations in wall temperature, Trans. ASME. 27 (1960) 241–249.

[21] R. Siegel, M. Perlmutter, Heat transfer for pulsating laminar duct flow, Heat Transfer 84 (1962) 111–122.

[22] Z. Guo, H. Sung, Analysis of the Nusselt number in pulsating pipe flow, Int. J. Heat Mass Transfer 40 (1997) 2486–2489.

[23] M. Faghri, K. Javdani, A. Faghri, Heat transfer with laminar pulsating flow in a pipe, Lett. Heat Mass Transfer 6 (1979) 259–270.

[24] S. Uchida, The pulsating viscous flow superposed on the steady laminar motion of incompressible fluid in a circular pipe, Z. Angew. Math. Phys. 7 (1956) 403–422.

[25] R. Siegel, Influence of oscillation diffusion on heat transfer in a uniformly heated channel, Trans. ASME 109 (1987) 244–249.

[26] H.N. Hemida, M.N. Sabry, a. Abdel-Rahim, H. Mansour, Theoretical analysis of heat transfer in laminar pulsating flow, Int. J. Heat Mass Transfer 45 (2002) 1767–1780.

[27] G.J. Brereton, Y. Jiang, Convective heat transfer in unsteady laminar parallel flows, Phys. Fluids. 18 (2006) 103602.

[28] D.a. Nield, a.V. Kuznetsov, Forced convection with laminar pulsating flow in a channel or tube, Int. J. Therm. Sci. 46 (2007) 551–560.

[29] T. Zhao, P. Cheng, A numerical solution of laminar forced convection in a heated pipe subjected to a reciprocating flow, Int. J. Heat Mass Transfer 38 (1995) 3011–3022.

[30] B.H. Yan, L. Yu, Y.H. Yang, Forced convection with laminar pulsating flow in a tube, Heat Mass Transfer 47 (2010) 197–202.

[31] M. Fakoor-Pakdaman, M. Andisheh-Tadbir, M. Bahrami, Transient internal forced convection under arbitrary time-dependent heat flux, in: Proc. ASME Summer Heat Transfer Conf., Minneapolis, MN, USA, 2013.

[32] M. Fakoor-Pakdaman, M. Andisheh-Tadbir, M. Bahrami, Unsteady laminar forced-convective tube flow under dynamic time-dependent heat flux, J. Heat Transfer 136 (2013) 041706-1–041706-10.

[33] E. Kreyszig, H. Kreyszig, E.J. Norminton, Advanced Engineering Mathematics, tenth ed., John Wiley & Sons, n.d.

[34] M. Fakoor-Pakdaman, M. Ahmadi, M. Bahrami, Unsteady internal forced-convective flow under dynamic time-dependent boundary temperature, J. Thermophys. Heat Transfer 28 (2014) 463–473.

[35] R. Siegel, M. Perlmutter, Laminar heat transfer in a channel with unsteady flow and wall heating varying with position and time, Trans. ASME 85 (1963) 358–365.

[36] T. Von Karman, M.A. Biot, Mathematical Methods in Engineering, McGraw-Hill, New York, 1940.

[37] R. Siegel, Forced convection in a channel with wall heat capacity and with wall heating variable with axial position and time, Int. J. Heat Mass Transfer 6 (1963) 607–620.

[38] A. Bejan, Convection Heat Transfer, third ed., USA, 2004.